Dentomaxillofacial Radiology (2016) 45, 20160228

birpublications.org/dmfr

RESEARCH ARTICLE

# Dose reduction potential of iterative reconstruction algorithms in neck CTA—a simulation study

[1]Stephan Ellmann, [1]Ferdinand Kammerer, [2]Thomas Allmendinger, [1]Michael Brand, [1]Rolf Janka, [1]Matthias Hammon, [3]Michael M Lell, [1]Michael Uder and [1]Manuel Kramer

*[1]Institute of Radiology, University Hospital Erlangen-Nuernberg, University of Erlangen-Nuernberg, Erlangen, Germany; [2]Siemens Healthineers GmbH, CT Division, Siemensstraße 1, Forchheim/Erlangen, Germany; [3]Clinicum Nuernberg, Department of Radiology and Nuclear Medicine, Paracelsus Medical University, Nuremberg, Germany*

**Objectives:** This study aimed to determine the degree of radiation dose reduction in neck CT angiography (CTA) achievable with Sinogram-affirmed iterative reconstruction (SAFIRE) algorithms.
**Methods:** 10 consecutive patients scheduled for neck CTA were included in this study. CTA images of the external carotid arteries either were reconstructed with filtered back projection (FBP) at full radiation dose level or underwent simulated dose reduction by proprietary reconstruction software. The dose-reduced images were reconstructed using either SAFIRE 3 or SAFIRE 5 and compared with full-dose FBP images in terms of vessel definition. 5 observers performed a total of 3000 pairwise comparisons.
**Results:** SAFIRE allowed substantial radiation dose reductions in neck CTA while maintaining vessel definition. The possible levels of radiation dose reduction ranged from approximately 34 to approximately 90% and depended on the SAFIRE algorithm strength and the size of the vessel of interest. In general, larger vessels permitted higher degrees of radiation dose reduction, especially with higher SAFIRE strength levels. With small vessels, the superiority of SAFIRE 5 over SAFIRE 3 was lost.
**Conclusions:** Neck CTA can be performed with substantially less radiation dose when SAFIRE is applied. The exact degree of radiation dose reduction should be adapted to the clinical question, in particular to the smallest vessel needing excellent definition.
*Dentomaxillofacial Radiology* (2016) **45**, 20160228. doi: 10.1259/dmfr.20160228

**Cite this article as:** Ellmann S, Kammerer F, Allmendinger T, Brand M, Janka R, Hammon M, et al. Dose reduction potential of iterative reconstruction algorithms in neck CTA—a simulation study. *Dentomaxillofac Radiol* 2016; **45**: 20160228.

**Keywords:** radiation dose; CT, spiral; angiography; carotid artery, external

## Introduction

In head and neck tumours, microvascular grafts are indispensable for reconstruction purposes following surgical resections or osteonecrosis of the mandible.[1]

The outcome of transplanted grafts is highly dependent on sufficient perfusion of the host vessels, which is in many cases either altered in terms of anatomic variants or impaired owing to prior surgery, tumour infiltration or radiation therapy. Additional atherosclerosis resulting from nicotine abuse as a known cause of oral cancer further affects therapeutic success negatively.

Thus, the perfusion of potential host vessels has to be determined prior to surgical reconstruction procedures and microvascular anastomoses. The imaging gold standard of selective intra-arterial angiography features risks of up to 1% for stroke, 4% for transient ischaemic attacks and almost 1% for death.[2–4] In recent years, conventional angiography has increasingly been replaced by MR angiography and CT angiography

Correspondence to: Dr Stephan Ellmann. E-mail: stephan.ellmann@uk-erlangen.de
University Hospital Erlangen—Department of Radiology is the main funder of this work.
Received 27 May 2016; revised 13 July 2016; accepted 25 July 2016

(CTA), involving substantially less risk for the above side effects.

While MR angiography is a method devoid of radiation, CTA includes substantial radiation dose application to the head and neck tissue, but offers higher spatial resolution along with surrounding bony structures as useful anatomical landmarks.[5,6]

CTA moreover has the advantage of being performed regularly in patients with cancer for staging purposes anyway, consequently offering "free insight" into the vessel situation of potential host vessels.

Several efforts have been taken to decrease the radiation dose level of CT and CTA examinations, including automatic dose level modulations, improved detector technologies, iterative reconstructions (IR) and several others.[7]

As a rule of thumb, performing CT examinations with reduced radiation dose impairs diagnostic image quality owing to an increase in image noise. IR techniques can be used to overcome these drawbacks by repeatedly performing the image reconstruction process, which leads to noise reduction. In an ideal setting, IR efforts fully compensate or even overcompensate the loss of image quality accompanying lower radiation dose application.

This radiation dose simulation study aimed to investigate the extent of possible radiation dose reduction in CTA of the external carotid artery (ECA) branches by determining the level of radiation dose reduction, at which dose-reduced iteratively-reconstructed CTA were considered indistinguishable from full-dose filtered back projections (FBPs) in terms of vessel definition.

## Methods and materials

*Patient examination*

This prospective single-centre study was approved by the institutional review board and complies with the Declaration of Helsinki. 10 consecutive patients (mean age 62.4 ± 10.5 years; 2 females, 8 males) scheduled for CTA of the supra-aortic vessels were prospectively included in this study. Written informed consent was obtained from all patients.

All examinations were performed on a 128-section CT system (Definition AS+; Siemens Healthineers GmbH, Erlangen, Germany), with a collimation of 128 × 0.6 mm and a pitch factor of 0.6. Attenuation-based tube current (mAs) modulation (CAREdose 4D) and tube voltage (kV) selection (CARE kV) were used. The image quality level was set to a reference value of 166 mAs at 120 kV, with the automatic kV adaption choosing 100 kV in all patients. The scan range included the head to the aortic arch. Circulation time was individually calculated by use of a test bolus injection with 10 ml of iodinated contrast medium at a flow rate of 5 ml $s^{-1}$, chased by a 50-ml saline bolus at the same flow rate. The region of interest to measure the time to peak was placed in the aortic arch. The delay of the diagnostic scan was calculated by use of the formula time to peak + 2 s. For the diagnostic scan, 50 ml of iodinated contrast medium and a subsequent 50-ml saline flush were used at the same flow rate of 5 ml $s^{-1}$.

The kV, mAs, CT dose index volume (in milligray) and dose–length product (in milligray × centimetres) were recorded from the patient protocol.

*Image reconstruction*

As repeated examinations of patients with different radiation dose levels are out of question owing to ethical reasons, this study relied on ReconCT, a proprietary image reconstruction software. ReconCT has repeatedly been demonstrated to be capable of simulating CT examinations including CTA with reduced mAs and thus reduced radiation dose levels by adding noise to the raw data prior to the reconstruction process.[7,8]

For dose simulation and reconstruction purposes, raw data were transferred to the ReconCT workstation, with the Sinogram-affirmed iterative reconstruction (SAFIRE) algorithm (Siemens Healthineers GmbH, Erlangen, Germany) used for IR.

Full-dose data sets were reconstructed with standard FBP and SAFIRE strength levels 3 and 5 without noise addition using a soft-tissue kernel (B31f for FBP and I31f for SAFIRE 3 and 5), resembling full-dose examinations. Following this procedure, dose reduction simulations were performed with 10–90% in steps of 10% of the original full-dose FBP with SAFIRE level settings of 3 and 5 and the same reconstruction kernels as above.

Reconstructed data sets of both FBP and IR were transferred to a workstation (syngo.via; Siemens Healthineers GmbH, Erlangen, Germany) in maximum intensity projection mode with a thickness of 10 mm, window width of 700 HU and window centre of 100 HU. In three patients, these windowing settings led to overcontrasted vessel structures, so that for these patients the window centre was set to 150 HU and the width to 900 HU. Arrows were added to sagittal images pointing on the ECA and its branches, classified according to their respective sizes: carotid bifurcation and main stem of the ECA (large); superior thyroid artery, lingual artery, facial artery, occipital artery, maxillary artery and superficial temporal artery (medium); and posterior auricular artery and ascending pharyngeal artery (small). The resulting images were exported in DICOM format.

A dedicated custom-made software tool presenting two images side by side on a PACS monitor (EIZO RadiForce RX650; Eizo, Hakusan, Japan) was used for image evaluation. One of these two images (randomly assigned to the monitor's left or right side) always constituted the full-dose FBP of a given vessel (defined by the arrow); the image on the other side always featured the identical vessel structure reconstructed iteratively with SAFIRE strength either 3 or 5 and radiation dose levels between 10 and 100% in steps of 10%.

**Table 1** Indecision point (IP) values for large, medium and small vessels reconstructed with either Sinogram-affirmed iterative reconstruction (SAFIRE) 3 or SAFIRE 5, along with 95% confidence intervals (CIs) and $R^2$ values of the sigmoid regression curves presented in Figure 1

| | *SAFIRE 3* | | | *SAFIRE 5* | | |
|---|---|---|---|---|---|---|
| | *IP* | *95% CI* | $R^2$ | *IP* | *95% CI* | $R^2$ |
| Large vessels | 23.7 | 23.0–24.5 | 0.9977 | 9.8 | 8.8–10.8 | 0.9748 |
| Medium vessels | 37.5 | 36.2–38.8 | 0.9965 | 25.3 | 23.0–27.5 | 0.9829 |
| Small vessels | 61.6 | 57.6–65.5 | 0.9797 | 66.0 | 61.6–70.3 | 0.9783 |

Five observers (four board-certified radiologists and one radiology resident with 4 years' experience in vascular imaging) were trained on the rating procedure with data sets not part of the study. The rating procedure was explained and the observers were asked to decide whether the marked vessel on the left or right side of the monitor featured superior definition and could be better demarcated by clicking on the image of choice (two alternative forced choice), leading to automatic data storage of the given answer and presentation of the next image pair. There were 3000 pairwise comparisons performed in total. Owing to the random image presentation and the random assignment to the two sides of the monitor, the observers could be considered blinded.

*Statistical analysis*

For large, medium and small vessels, every radiation dose level was analyzed separately to determine in how many cases the dose-reduced iteratively reconstructed image was preferred by the observers and in how many cases the full-dose FBP of the similar anatomical structure received superior rating. From these numbers, the quotient ["preference ratio" (PR)] was calculated, with a PR of 1 depicting the absolute preference of the observers for the iteratively reconstructed image at a given dose level and a PR of 0 depicting the preference for the full-dose FBP.

A PR of 0.5 thus states that the observers can be considered to be uncertain whether the full-dose FBP or the dose-reduced iteratively reconstructed image featured superior vessel definition—picking one or the other image in 50% each. Thus, the corresponding radiation dose level (%) to a PR of 0.5 will be referred to as "indecision point" (IP). The radiation dose reduction potential can be calculated with the formula 100% − IP.

Interobserver agreement was determined by calculating the percentage of agreement; Cohen's and Fleiss' kappa and interpreted as follows: values $< 0$, no agreement; 0–0.20, slight; 0.21–0.40, fair; 0.41–0.60, moderate; 0.61–0.80, substantial; 0.81–1, almost perfect agreement.

Resulting data were plotted into diagrams, with the radiation dose levels on the axis of abscissae and the PR on the axis of ordinates. This was performed for small, medium and large vessels and SAFIRE 3 and SAFIRE 5 separately. Best fit curves were calculated from the data points of each diagram by the use of the formula $Y = x^n/(\mathrm{IP}^n + x^n)$. The values for IP and $n$ were calculated with 1000 iteration steps for curve fitting and optimized for least-squares ordinary fit. In addition, 95% confidence interval (CI) envelopes were calculated and $R^2$ was determined for goodness of fit quantification.

The IPs of different sigmoid curves were compared with each other by the means of extra sum-of-squares $F$-tests. In all statistical tests, $p$-values $<0.05$ were considered statistically significant.

## Results

*Scan parameters*

Examinations were performed with an average CT dose index volume of $7.13 \pm 0.72$ mGy, a respective dose–length product of $231.80 \pm 29.30$ mGy × cm and an effective radiation dose of 1.18 mSv ($k$-factor 0.0051).[9]

*Interobserver agreement*

Fleiss' kappa as a measure of interobserver agreement was 0.66, resulting from an overall interobserver agreement of 84.2%. Individual Cohen's kappa values ranged from 0.596 to 0.709.

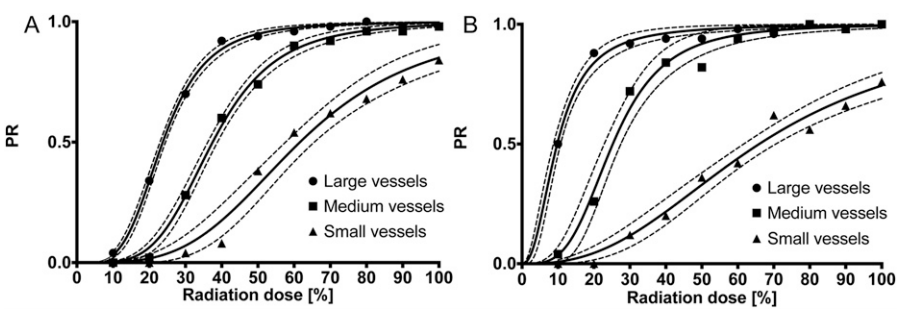


**Figure 1** Regression curves for large, medium and small vessel images reconstructed with either Sinogram-affirmed iterative reconstruction (SAFIRE) 3 (a) or SAFIRE 5 (b). The radiation dose level (%) is presented on the axis of abscissae and the preference ratio (PR) on the axis of ordinates. The thinner dotted lines indicate 95% confidence intervals.

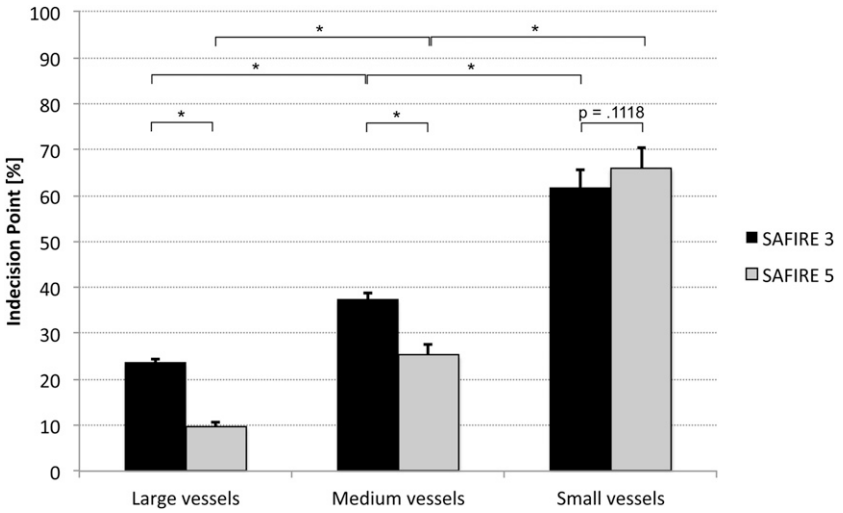


**Figure 2** Indecision points of large, medium and small vessels, dependent on Sinogram-affirmed iterative reconstruction (SAFIRE) strength (3 *vs* 5). While SAFIRE 5 is significantly superior to SAFIRE 3 concerning large and medium vessels ($p < 0.0001$), this advantage is lost in terms of small vessels ($p = 0.1118$).

*Determination of the Sinogram-affirmed iterative reconstruction dose reduction potential*

The regression curves adequately modelled reality with all $R^2$ values $\geq 0.9748$ (Table 1).

SAFIRE 3 and 5 regression curves differed significantly from each other (Figure 1) (all $p$-values $<0.0023$). The values of the IPs along with their 95% CIs are depicted in Figure 2 and a numerical presentation is shown in Table 1. Notably, no significant difference was observed between the IPs of SAFIRE 3 and 5 for small vessels ($p = 0.1118$), whereas the IPs of SAFIRE 3 and 5 significantly differed for medium and large vessels. A direct effect of this finding is presented in Figure 3. While the vessel definition of the carotid bifurcation is maintained in the SAFIRE images at their respective large-vessel IPs, the vessel definition of the ascending pharyngeal artery gradually decreases from FBP over SAFIRE 3 to SAFIRE 5. A generalized impression of different radiation dose levels (including the IPs) for medium vessels is exemplified through the occipital artery in Figure 4.

## Discussion

This study aimed to investigate the radiation dose reduction potential of SAFIRE in CTA of the ECA branches using two alternative forced choice comparisons. The potential levels of dose reduction depended highly on the sizes of the vessels of interest, as well as on the strength of the SAFIRE algorithm (Table 1, Figures 1 and 2).

SAFIRE, to a certain extent, can counterbalance the increased image noise that accompanies imaging with reduced mAs and thus reduced radiation dose, but at the price of blotchy or plastic-like image appearance

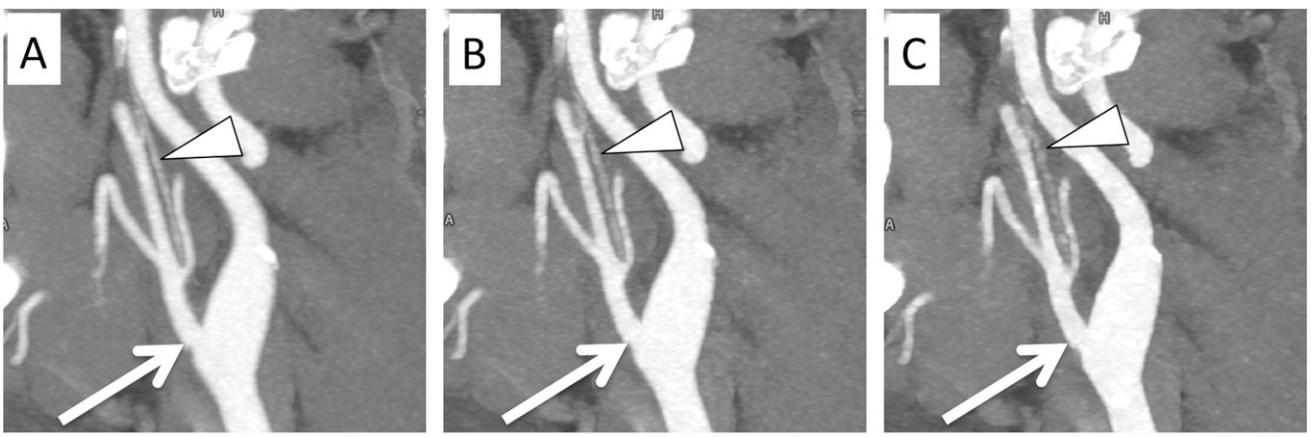


**Figure 3** Sagittal maximum intensity projections of the carotid bifurcation (arrows) in a 100% filtered back projection (a) and in Sinogram-affirmed iterative reconstruction (SAFIRE) 3 (b) and SAFIRE 5 (c) at their indecision points of 24 and 10%, respectively. The decreasing quality of the vessel definition of the ascending pharyngeal artery (arrowheads) from left to right can be noted.

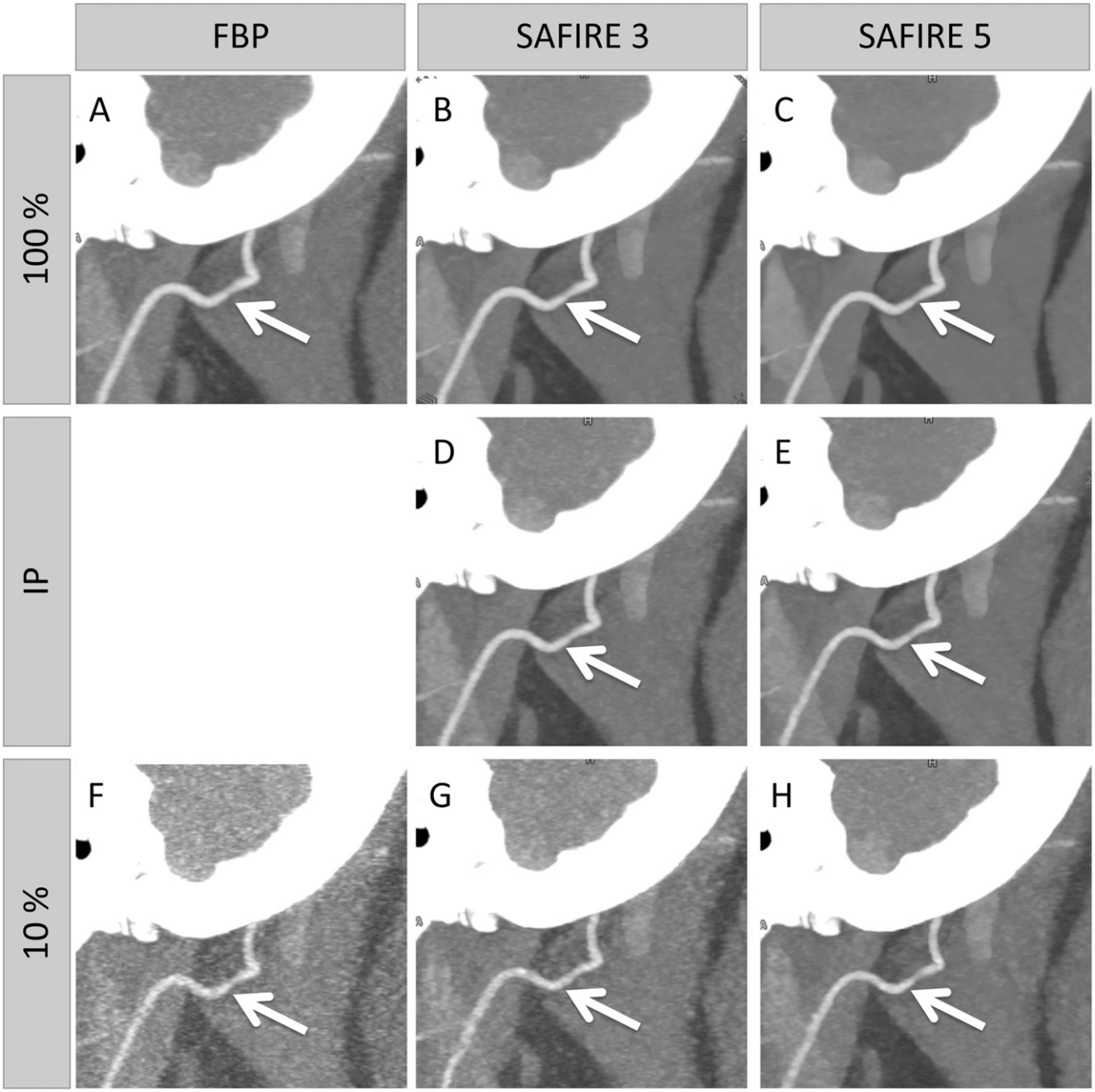


**Figure 4** Exemplary sagittal maximum intensity projection reconstructions with focus on the occipital artery at 100% radiation dose level in filtered back projection (FBP) (a) and reconstructed iteratively with Sinogram-affirmed iterative reconstruction (SAFIRE) 3 (b) and SAFIRE 5 (c). In addition, SAFIRE 3 and SAFIRE 5 iterative reconstructions are shown at their indecision points (IPs) of 38% (d) and 25% (e), respectively, as well as FBP and SAFIRE reconstructions at radiation dose levels of 10% (f–h).

most apparent on SAFIRE images with high IR strengths.[10,11] This becomes increasingly important for smaller vessel structures.

The results of this study are mainly in line with a former study investigating intracranial vessels,[7] with larger vessels yielding higher dose reduction potentials than smaller ones.

In terms of the dependence on SAFIRE strength, SAFIRE 5 featured significantly lower IPs in large and medium neck vessels (9.8 *vs* 23.7% and 25.3 *vs* 37.5%, respectively), thus allowing significantly higher rates of radiation dose reduction. Interestingly, this significant advantage of SAFIRE 5 over SAFIRE 3 was lost in terms of small vessel visualization (ascending pharyngeal artery and posterior auricular artery, $p = 0.1118$).

The relatively high levels of potential dose reduction of up to 90% in large vessels can be explained by the fact that in CTA, high-contrasted structures are evaluated.

These objects offer *per se* higher contrast-to-noise ratio and signal-to-noise ratio that can be further improved by SAFIRE.[10,12,13] In addition, the larger the object (*i.e.* a vessel), the easier the definition of its outlines by an iterative algorithm.[14] This nonetheless holds true only for sufficiently large vessels, in which the pixelated appearance of images with higher IR strengths[10,11] does not necessarily influence the visual impression as a whole. With smaller vessels such as the ascending pharyngeal artery or the posterior auricular artery, the non-linearity of the SAFIRE algorithm becomes increasingly relevant. This non-linearity results in a more prominent shift of the noise–power–spectrum peak to the left with increasing SAFIRE strengths, leading to increased noise reduction at the expense of spatial resolution.[15]

Thus, while both SAFIRE 3 and 5 still provide remarkable dose reduction potential in CTA, the superiority of SAFIRE 5 over 3 vanishes for small vessels (Figures 2 and 4).

Interestingly, the above-mentioned non-linearity is also reflected in the sigmoidal shape of the regression curves (Figure 1) and in the width of the IP CIs, being narrow for large vessels and wide for small vessels.

This study provides clear evidence for a strong dependence of SAFIRE dose reduction potentials on the size of the vessel of interest, ranging from approximately 34% for small vessels to approximately 90% for large vessels. Former studies mainly focused on image impression as a whole and showed 20.9% dose reduction potential for adaptive statistical iterative reconstruction[16] in neck CTA and 17% for soft-tissue CT.[17] Advanced Modeled Iterative Reconstruction allowed radiation dose reductions of up to 34% in neck soft-tissue CT while increasing image quality.[18]

The results of this study imply dose reduction strategies according to the clinical setting and radiologist preferences. A reasonable approach is to strive for excellent definition of small vessels, consequently reduce the radiation dose by about 38% and use SAFIRE 3 as an IR algorithm.

Another arguable strategy is to abstain from excellent definition of small vessels (as they are inappropriate for flap anastomoses anyway[19]) and rather concentrate on excellent vessel definition of medium vessels, allowing radiation dose reductions of up to about 62% in case of SAFIRE 3. In this case, an even higher grade of reduction could be achieved by the use of SAFIRE 5 (up to about 75%), at the cost of a slightly blotchy image impression possibly unfamiliar to some radiologists.

Limitations of this study include the fact that reduced radiation dose was simulated by lowering mAs. Although this simulation has been proven to be extremely reliable,[7] it cannot be guaranteed that this method of radiation dose reduction can be directly translated to different dose reduction strategies. One very interesting additional strategy would be the modification of kV parameters, as a kV closer to the *k* edge of iodine at 33 keV can have beneficial effects on both radiation dose and image quality.[20] Yet, to the best of our knowledge, no simulation software exists allowing a simulation of scans with decreased kV or a combination of modified voltages and currents.

## Conclusions

Taken together, this study adds to the increasing field of radiation dose reduction strategies in CT examinations and may help users gain the confidence for lowering routine dose levels. Although CT dose reduction strategies to prevent cancerogenesis might be considered less important in patients having undergone radiation therapy, the as low as reasonably achievable (ALARA) principle should still be followed.

## References

1. Kramer M, Schwab SA, Nkenke E, Eller A, Kammerer F, May M, et al. Whole body magnetic resonance angiography and computed tomography angiography in the vascular mapping of head and neck: an intraindividual comparison. *Head Face Med* 2014; **10**: 16. doi: https://doi.org/10.1186/1746-160X-10-16
2. Davies KN, Humphrey PR. Complications of cerebral angiography in patients with symptomatic carotid territory ischaemia screened by carotid ultrasound. *J Neurol Neurosurg Psychiatry* 1993; **56**: 967–72.
3. Hankey GJ, Warlow CP, Molyneux AJ. Complications of cerebral angiography for patients with mild carotid territory ischaemia being considered for carotid endarterectomy. *J Neurol Neurosurg Psychiatry* 1990; **53**: 542–8.
4. Johnston DC, Chapman KM, Goldstein LB. Low rate of complications of cerebral angiography in routine clinical practice. *Neurology* 2001; **57**: 2012–14. doi: https://doi.org/10.1212/WNL.57.11.2012
5. Cappabianca S, Scuotto A, Iaselli F, Pignatelli di Spinazzola N, Urraro F, Sarti G, et al. Computed tomography and magnetic resonance angiography in the evaluation of aberrant origin of the external carotid artery branches. *Surg Radiol Anat* 2012; **34**: 393–9. doi: https://doi.org/10.1007/s00276-011-0926-3
6. Lell M, Tomandl BF, Anders K, Baum U, Nkenke E. Computed tomography angiography versus digital subtraction angiography in vascular mapping for planning of microsurgical reconstruction of the mandible. *Eur Radiol* 2005; **15**: 1514–20. doi: https://doi.org/10.1007/s00330-005-2770-5
7. Ellmann S, Kammerer F, Brand M, Allmendinger T, May MS, Uder M, et al. A novel pairwise comparison-based method to determine radiation dose reduction potentials of iterative reconstruction algorithms, exemplified through circle of willis computed tomography angiography. *Invest Radiol* 2016; **51**: 331–9.
8. Kramer M, Ellmann S, Allmendinger T, Eller A, Kammerer F, May MS, et al. Computed tomography angiography of carotid arteries and vertebrobasilar system: a simulation study for radiation dose reduction. *Medicine (Baltimore)* 2015; **94**: e1058. doi: https://doi.org/10.1097/MD.0000000000001058
9. Deak PD, Smal Y, Kalender WA. Multisection CT protocols: sex- and age-specific conversion factors used to determine effective dose from dose-length product. *Radiology* 2010; **257**: 158–66. doi: https://doi.org/10.1148/radiol.10100047
10. Kalra MK, Woisetschlager M, Dahlstrom N, Singh S, Lindblom M, Choy G, et al. Radiation dose reduction with sinogram

affirmed iterative reconstruction technique for abdominal computed tomography. *J Comput Assist Tomogr* 2012; **36**: 339–46. doi: https://doi.org/10.1097/RCT.0b013e31825586c0
11. Yu MH, Lee JM, Yoon JH, Baek JH, Han JK, Choi BI, et al. Low tube voltage intermediate tube current liver MDCT: sinogram-affirmed iterative reconstruction algorithm for detection of hypervascular hepatocellular carcinoma. *AJR Am J Roentgenol* 2013; **201**: 23–32. doi: https://doi.org/10.2214/AJR.12.10000
12. Schabel C, Fenchel M, Schmidt B, Flohr TG, Wuerslin C, Thomas C, et al. Clinical evaluation and potential radiation dose reduction of the novel sinogram-affirmed iterative reconstruction technique (SAFIRE) in abdominal computed tomography angiography. *Acad Radiol* 2013; **20**: 165–72. doi: https://doi.org/10.1016/j.acra.2012.08.015
13. Yang WJ, Yan FH, Liu B, Pang LF, Hou L, Zhang H, et al. Can sinogram-affirmed iterative (SAFIRE) reconstruction improve imaging quality on low-dose lung CT screening compared with traditional filtered back projection (FBP) reconstruction? *J Comput Assist Tomogr* 2013; **37**: 301–5. doi: https://doi.org/10.1097/RCT.0b013e31827b8c66
14. Chen B, Ramirez Giraldo JC, Solomon J, Samei E. Evaluating iterative reconstruction performance in computed tomography. *Med Phys* 2014; **41**: 121913. doi: https://doi.org/10.1118/1.4901670
15. Ehman EC, Yu L, Manduca A, Hara AK, Shiung MM, Jondal D, et al. Methods for clinical evaluation of noise reduction techniques in abdominopelvic CT. *Radiographics* 2014; **34**: 849–62. doi: https://doi.org/10.1148/rg.344135128
16. Komlosi P, Zhang Y, Leiva-Salinas C, Ornan D, Patrie JT, Xin W, et al. Adaptive statistical iterative reconstruction reduces patient radiation dose in neuroradiology CT studies. *Neuroradiology* 2014; **56**: 187–93. doi: https://doi.org/10.1007/s00234-013-1313-z
17. Vachha B, Brodoefel H, Wilcox C, Hackney DB, Moonis G. Radiation dose reduction in soft tissue neck CT using adaptive statistical iterative reconstruction (ASIR). *Eur J Radiol* 2013; **82**: 2222–6. doi: https://doi.org/10.1016/j.ejrad.2013.08.014
18. Scholtz JE, Wichmann JL, Husers K, Albrecht MH, Beeres M, Bauer RW, et al. Third-generation dual-source CT of the neck using automated tube voltage adaptation in combination with advanced modeled iterative reconstruction: evaluation of image quality and radiation dose. *Eur Radiol* 2016; **26**: 2623–31. doi: https://doi.org/10.1007/s00330-015-4099-z
19. Kramer M, Nkenke E, Kikuchi K, Schwab SA, Janka R, Uder M, et al. Whole-body magnetic resonance angiography for presurgical planning of free-flap head and neck reconstruction. *Eur J Radiol* 2012; **81**: 262–6. doi: https://doi.org/10.1016/j.ejrad.2010.11.016
20. Meyer M, Haubenreisser H, Schoepf UJ, Vliegenthart R, Leidecker C, Allmendinger T, et al. Closing in on the K edge: coronary CT angiography at 100, 80, and 70 kV-initial comparison of a second- *versus* a third-generation dual-source CT system. *Radiology* 2014; **273**: 373–82. doi: https://doi.org/10.1148/radiol.14140244